Performance of the Space-Time Block Coded DS-CDMA Uplink Employing Soft-Output ACO-Aided Multiuser Space-Time Detection and Iterative Decoding

Chong Xu, Mohammed El-Hajjar, Rob G Maunder, Lie-Liang Yang and Lajos Hanzo
School of ECS., Univ. of Southampton, SO17 1BJ, UK.
Tel: +44-23-80-593 125, Fax: +44-23-80-593 045
Email: {cx05r, lly, lh}@ecs.soton.ac.uk, http://www-mobile.ecs.soton.ac.uk

***Abstract*—In this treatise we propose a three-stage twin-transmit-antenna assisted MultiUser (MU) Direct Sequence Code-Division Mulitple Access (DS-CDMA) system employing both a Unitary Rate Code (URC) and a Recursive Systematic Code (RSC) to carry out iterative turbo detection. A Space-Time Block Code (STBC) is used to provide second-order diversity gain in conjunction with a novel soft-output (SO) ant-colony-optimization (ACO) based space-time multiuser detection (ST/MUD) algorithm, which is capable of carrying out STBC decoding, while mitigating the MultiUser Interference (MUI) and generating the Log-Likelihood Ratios (LLR) for facilitating the iterative exchange of extrinsic information between the URC and RSC decoders of each user. With aid of the above mentioned state-of-the-art techniques, the proposed system becomes capable of approaching the performance of the single-user system within about 0.5dB, when $K = 32$ users are supported with the aid of 31-chip Gold-codes.**

I. Introduction

Ant-Colony Optimization (ACO) [1] was inspired by the foraging behavior of the ant-colony in nature. The first ACO based MUD algorithm was introduced by Hijazi in 2004 [2]. When initialized by the Matched Filter's (MF) outputs, the ACO algorithm converges to the optimal binary solution, despite calculating the objective function of the entire legitimate set of 2^K solutions. This algorithm was reported to have a better bit-error ratio (BER) performance a the corresponding Genetic Algorithm (GA) aided MUD [2]. In 2008, Xu *et al.* proposed the first soft-output (SO) ACO based MUD algorithm [3], [4] that is capable of providing the log-likelihood ratio (LLR) of each bit in the MU DS-CDMA system. This SO MUD was reported to enable the MU system to approach the channel-coded single user performance at a complexity that was found to be a factor of 10^8 lower than that of the optimum Bayesian MUD a $K = 32$-user the DS CDMA system.

In this treatise, we will propose a novel SO/ACO based space-time (ST) MUD algorithm, which jointly carries out STBC decoding for each user and simultaneously mitigates the multiuser-interference, while achieving a second-order diversity gain. We will demonstrate that the proposed algorithm will enable the multi-user system to approach the single-user performance at a significanly reduced complexity, which is a factor 10^{17} lower than that of the Bayesian MUD for a $K = 32$-user system.

The assumption of having independent fading for the two transmit antennas of shirt-pocket-sized communicator is unrealistic. However, assuming an antenna-separation of say 30 cm, i.e. two wavelengths at 2 GHz in a laptop transmitter might provide sufficient decorrelation for approching our idealized assumption of having independent fading. Alternatively, two single-antenna-aided mobiles may form a distributed $\mathcal{G}_2$ space-time code, which would have a near-perfect relay-link between them. Naturallly, this requires the creation of two time - or frequency - slots for the classic broadcast-phase and cooperation-phase of the mobiles, as detailed in [5], hence potentially halving the total system's throughput in exchange for the $\mathcal{G}_2$-STBC based 2nd-order diversity.

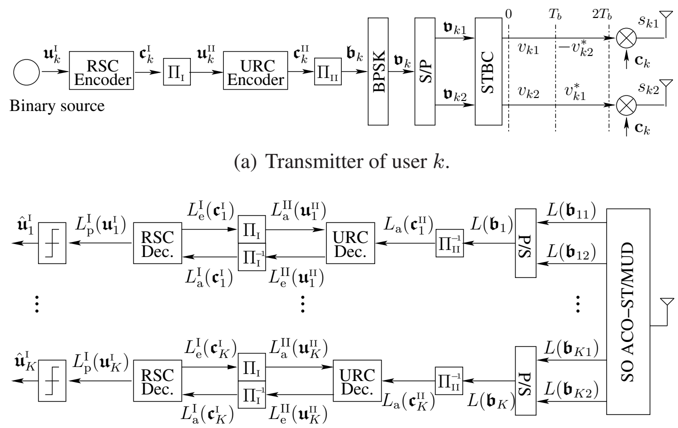

(a) Transmitter of user k.

(b) Receiver at the BS.

Fig. 1: Schematic diagram of a DS-CDMA uplink employing RSC, URC, STBC, space-time multiuser detection as well as iterative decoding.

On the other hand, in order to achieve a near-capacity performance, typically channel coding is used and iterative decoding may be employed to exchange extrinsic information between the receiver modules. In [6] an iteratively detected scheme was proposed for the Rayleigh fading MIMO channel, where an orthogonal STBC scheme was considered as the inner code combined with an additional block code as the outer channel code. It was demonstrated in [7] that a recursive inner code is needed in order to avoid the formation of a Bit Error Ratio (BER) floor, when employing iterative decoding. In [8], unity-rate inner codes were employed for designing low complexity turbo codes suitable for bandwidth and power limited systems having stringent BER requirements.

The rest of the paper is organized as follows. In Section II, the system's architecture is characterized. The SO/ACO based ST/MUD algorithm is described in Section III. The BER performance of the proposed system and our complexity estimates are characterized in Section IV. Finally, our conclusions are provided in Section V.

II. System Description

The DS-CDMA uplink studied in this contribution is shown in Fig. 1. More specifically, the block diagram of the mobile transmitter of the kth user and the base-station's (BS) receiver are depicted in Fig. 1(a) and Fig. 1(b), respectively. Below, we will use calligraphic characters to represent the vector containing all the bits/symbols transmitted or received by user k during a certain transmitted frame, such as in $\mathfrak{c}_k^{\mathrm{I}}$. Furthermore, we will use bold characters to represent the vector or matrix containing all the elements associated with either a specific user or with all the K users, within a STBC block duration, a symbol duration or a chip interval.

As shown in Fig. 1(a), the N_{u}-bit source bit stream $\mathbf{u}_k$ of the kth user, $k = 1, 2, \ldots, K$ is first encoded by a 1/2-rate Recursive Systematic Convolutional (RSC) code, yielding the N_{c}-bit RSC coded bit stream $\mathfrak{c}_k^{\mathrm{I}}$. Then it is interleaved by the random bit interleaver Π_{I} of Fig. 1(a) providing the output bit stream $\mathfrak{u}_k^{\mathrm{II}}$. The bit stream $\mathfrak{u}_k^{\mathrm{II}}$ is then further encoded by a Unity-Rate Code (URC), generating the coded bit stream $\mathfrak{c}_k^{\mathrm{II}}$. After passing through another random bit interleaver Π_{II}, the interleaved URC coded bit stream $\mathfrak{b}_k$ is then a binary phase-shift keying (BPSK) modulated, yielding the symbol stream $\mathfrak{v}_k$. Finally, after serial-to-parallel (S/P) conversion, the parallel $N_{\mathrm{c}}/2$-length symbol streams $\mathfrak{v}_{k1}$ and $\mathfrak{v}_{k2}$ of Fig. 1(a) are rearranged by the $\mathcal{G}_2$ space-time coding scheme [10], yielding the N_{c}-length symbol stream. Then each of the two parallel symbol streams is direct-sequence spread employing the N_{s}-chip user-specific quasi-orthogonal spreading sequence $\mathbf{c}_k$. The $(N_{\mathrm{s}}\times N_{\mathrm{c}})$-chip signal streams of a user are transmitted to the BS from two transmit antennas.

Let assume for simplicity that the signals are transmitted to the BS over non-dispersive, slowly fading channels, which exhibit a constant envelope over a STBC block duration. Then, it can be shown that the received complex-valued observations obtained from the $2N_{\mathrm{s}}$ chip durations of a STBC period can be written as

$$\mathbf{r} = \xi \mathbf{C}\mathbf{H}\mathbf{v} + \mathbf{n}, \tag{1}$$

where $\xi{=}1/\sqrt{2N_{\mathrm{s}}}$ is a normalization factor, $\mathbf{C}{=}[\mathbf{C}_1, \mathbf{C}_2,\cdots,\mathbf{C}_K]$ obeying $\mathbf{C}_k = \mathbf{c}_k \otimes \mathbf{I}_2$, where $\mathbf{c}_k$ is the kth user's spreading sequence, $\mathbf{I}_2$ is a (2×2)-element identity matrix and $\otimes$ denotes the *Kronecker product* operation. Furthermore, we have $\mathbf{H} = \mathrm{diag}\{\mathbf{H}_1, \mathbf{H}_2, \cdots, \mathbf{H}_K\}$ in (1), where

$$\mathbf{H}_k = \begin{bmatrix} h_{k1} & h_{k2} \\ h_{k2}^* & -h_{k1}^* \end{bmatrix} \tag{2}$$

accounts for the space-time fading channels, $\mathbf{v} = \left[\mathbf{v}_1^T, \mathbf{v}_2^T, \ldots, \mathbf{v}_K^T\right]^T$ associated with $\mathbf{v}_k = [v_{k1}, v_{k2}]^T$ contains the $2K$ transmitted coded bits and, finally, $\mathbf{n} = \left[\mathbf{n}_1^T, \mathbf{n}_2^H\right]^T$ associated with $\mathbf{n}_\jmath = [n_{\jmath1}, n_{\jmath2}, \cdots, n_{\jmath N_{\mathrm{s}}}]^T$, $\jmath = 1, 2$, denotes the complex-valued Gaussian noise samples, which have a zero mean and a common variance of $\frac{1}{2}\sigma_{\mathrm{N}}^2 = N_0/[2E_{\mathrm{b}}(\mathfrak{b})] = N_0/[E_{\mathrm{b}}(\mathfrak{u}^{\mathrm{I}})]$ in both the real and imaginary component of $\mathfrak{n}$, where E_{b} is the energy per URC coded bit.

The extrinsic soft information, quantified in terms of Logarithmic Likelihood Ratios (LLR) is iteratively exchanged between the URC and the RSC decoder. In Fig. 1(b), $L(\cdot)$ denotes the LLRs of the bits concerned, where the superscript 'I' or 'II' indicates the first and the second decoder, namely the RSC and URC decoders. Additionally, the subscript 'a', 'p' and 'e' represent the *a priori*, *a posteriori* and extrinsic information, respectively.

As shown in Fig. 1(b), the observation vector $\mathbf{r}$ received during a STBC block interval is first input to the SO-ACO/ST-MUD, which generates the $(2K \times 1)$-element soft output vector $\mathbf{L}$ containing the LLRs of all the $2K$ bits transmitted during a STBC block interval. After receiving the $N_{\mathrm{c}}/2$ $2K$-element vectors output from the SO-ACO/ST-MUD during the $N_{\mathrm{c}}/2$ STBC block duration, the $2K$ LLR streams $L(\mathfrak{b}_{11})$, …, $L(\mathfrak{b}_{K2})$ comprising the $(N_{\mathrm{c}} \times K)$ number of LLRs associated with all the $(N_{\mathrm{c}} \times K)$ bits transmitted by all the K users during a transmission frame interval are input into the K P/S converters of Fig. 1(b) and are converted back to K number of LLR streams $L(\mathfrak{b}_1)$, …, $L(\mathfrak{b}_K)$. As shown in Fig. 1(b) for the kth user $k = 1, \ldots, K$, the extrinsic LLR stream $L(\mathfrak{b}_k)$ generated by the SO ACO-based ST-MUD is first deinterleaved by the second random soft-bit deinterleaver Π_{II}^{-1}, yielding $L_{\mathrm{a}}^{\mathrm{II}}(\mathfrak{c}_k^{\mathrm{II}})$. Then the URC decoder processes the LLR values $L_{\mathrm{a}}^{\mathrm{II}}(\mathfrak{c}_k^{\mathrm{II}})$ of the URC-encoded bit stream $\mathfrak{c}_k^{\mathrm{II}}$ in combination with the LLR stream $L_{\mathrm{a}}^{\mathrm{II}}(\mathfrak{u}_k^{\mathrm{II}})$ containing the *a priori* LLR values of the uncoded bit stream $\mathfrak{u}_k^{\mathrm{II}}$ of Fig. 1(b) in order to generate the extrinsic LLR values of the uncoded bit stream $\mathfrak{u}_k^{\mathrm{II}}$ at the input of the URC, yielding the LLR stream $L_{\mathrm{e}}^{\mathrm{II}}(\mathfrak{u}_k^{\mathrm{II}})$. Then, the extrinsic LLR stream $L_{\mathrm{e}}^{\mathrm{II}}(\mathfrak{u}_k^{\mathrm{II}})$ is deinterleaved by the first random soft-bit deinterleaver Π_{I}^{-1} of Fig. 1(b), yielding the deinterleaved LLR stream $L_{\mathrm{a}}^{\mathrm{I}}(\mathfrak{c}_k^{\mathrm{I}})$, which constitutes at the same time the *a priori* LLR stream of the RSC coded bits $\mathfrak{c}_k^{\mathrm{I}}$.

Next, the *a priori* LLR values of the RSC coded bit stream $\mathfrak{c}_k^{\mathrm{I}}$ represented by $L_{\mathrm{a}}^{\mathrm{I}}(\mathfrak{c}_k^{\mathrm{I}})$ are input to the RSC decoder in order to generate the extrinsic LLR values for the RSC coded bit stream $\mathfrak{c}_k^{\mathrm{I}}$ of Fig. 1(b), yielding $L_{\mathrm{e}}^{\mathrm{I}}(\mathfrak{c}_k^{\mathrm{I}})$. After appropriately reordering the LLR values by the first soft-bit interleaver Π_{I}, the interleaved LLR stream $L_{\mathrm{a}}^{\mathrm{II}}(\mathfrak{u}_k^{\mathrm{II}})$ is then fed back to the URC decoder in conjunction with the *a priori* LLR values of all the URC coded bits $L_{\mathrm{a}}(\mathfrak{c}_k^{\mathrm{II}})$ of Fig. 1(b) to generate the extrinsic LLR values $L_{\mathrm{e}}^{\mathrm{II}}(\mathfrak{u}_k^{\mathrm{II}})$ for all the uncoded bits $\mathfrak{u}_k^{\mathrm{II}}$ at the input of the URC during the second iteration. Again, after being passed through the second random soft-bit deinterleaver Π_{I}^{-1}, the deinterleaved LLR stream $L_{\mathrm{a}}^{\mathrm{I}}(\mathfrak{c}_k^{\mathrm{I}})$ is input to the RSC decoder as the *a priori* information of the coded bits $\mathfrak{c}_k^{\mathrm{I}}$ during the second iteration.

As for the RSC decoder's action during the last iteration, instead of the extrinsic LLR values of the coded bits $L_{\mathrm{e}}^{\mathrm{I}}(\mathfrak{c}_k^{\mathrm{I}})$, only the stream $L_{\mathrm{p}}^{\mathrm{I}}(\mathfrak{u}_k^{\mathrm{I}})$ of Fig. 1(b) containing the *a posteriori* LLR values of all the original uncoded binary source bits $\mathfrak{u}_k^{\mathrm{I}}$ are required. More explicitly, the *a posteriori* LLR values $L_{\mathrm{p}}^{\mathrm{I}}(\mathfrak{u}_k^{\mathrm{I}})$ are then fed into the hard-output decision device of Fig. 1(b) in order to determine the final detection output for the binary source bit stream $\mathfrak{u}_k^{\mathrm{I}}$ of the kth user.

III. Soft-Output ACO-Aided Space-Time Multiuser Detection

A. Derivation of the LLRs

The LLR value $L(\mathfrak{b}_{k\imath})$ of Fig. 1(b) associated with the $\imath$th symbol for $\imath = 1$ or 2 and transmitted by the kth user for $k = 1, \ldots, K$ within a certain STBC block duration is denoted as $L_{k\imath}$ for simplicity, which is defined by [12]

$$L_{k\imath} = \ln \frac{P(v_{k\imath} = +1|\mathbf{r}, \mathbf{H})}{P(v_{k\imath} = -1|\mathbf{r}, \mathbf{H})}, \imath = 1, 2 \qquad k = 1, 2, \ldots, K. \tag{3}$$

Upon applying the Bayesian rule of probability [13] and assuming that both the *a priori* probabilities of 0 and 1 in the binary source are 0.5, Eq. (3) can be further expressed as

$$L_{k\imath}^{\mathrm{Bay}} = \ln \frac{\sum_{\mathbf{v}_{M,i}^{(\kappa+)} \in \mathbb{V}_M^{(\kappa+)}} p(\mathbf{r}|\mathbf{v}_{M,i}^{(\kappa+)}, \mathbf{H})}{\sum_{\mathbf{v}_{M,i}^{(\kappa-)} \in \mathbb{V}_M^{(\kappa-)}} p(\mathbf{r}|\mathbf{v}_{M,i}^{(\kappa-)}, \mathbf{H})}, \quad i = 1, \ldots, \frac{\mathcal{M}}{2}, \qquad \text{subject to } \kappa = 2(k-1) + \imath, \tag{4}$$

where $M = 2K$ denotes the number of elements in each vector and $\mathcal{M} = 2^M = 2^{2K}$ is the cardinality of the full set containing all the legitimate vectors of the M-symbol BPSK modulated binary source combinations. Furthermore, $\mathbf{v}_{M,i}^{(\kappa)+}$ in Eq. (4) defines the set containing the $(\mathcal{M}/2)$ vectors having the κth symbol given by $+1$. The index κ in Eq. (4) is an integer ranging from 1 to $2K$ and v_κ in the $2K$-element vector $\mathbf{v}$ represents the same element as v_{ki} iff we have $\kappa = 2(k-1) + i$.

In Eq. (1) the $2N_s$-element AWGN vector $\mathbf{n}$ having elements $n_{\jmath n_s}$ for $\jmath = 1, 2$ and $n_s = 1, 2, \ldots, N_s$ is an instantaneous sample of the complex-valued Gaussian random variable $\mathfrak{n}$ having a mean of $\mu_\mathfrak{n} = 0$ and a variance of $\sigma_\mathfrak{n}^2 = N_0/E_b(\mathfrak{b})$. In other words, we have $n_{\jmath n_s} \sim \mathcal{N}^c(\mu_\mathfrak{n}, \sigma_\mathfrak{n}^2)$. According to [13], the PDF of the d-dimensional complex Gaussian variable $\mathbf{n} \sim \mathcal{N}_d^c(\mathbf{M}_\mathfrak{n}, \boldsymbol{\Sigma}_\mathfrak{n})$ is given by

$$p(\mathbf{n}) = \frac{1}{\pi^d} \frac{\exp\left[-\frac{1}{2}(\mathbf{n} - \mathbf{M}_\mathfrak{n})^H 2\boldsymbol{\Sigma}_\mathfrak{n}^{-1}(\mathbf{n} - \mathbf{M}_\mathfrak{n})\right]}{\det(\boldsymbol{\Sigma}_\mathfrak{n})}. \qquad (5)$$

In Eq.(5), the number of elements in the random vector is $2N_s$, while the vectors $\mathbf{M}_\mathfrak{n}$ and $\boldsymbol{\Sigma}_\mathfrak{n}$ represent the mean vector and the variance vector, containing the mean and variance of each random variable element of $\mathbf{n}$, which can be defined as

$$\begin{aligned} \mathbf{M}_\mathfrak{n} &= \mathbf{0}^{(2N_s)}; \quad d = 2N_s \\ \boldsymbol{\Sigma}_\mathfrak{n} &= E\left((\mathbf{n} - \mathbf{M}_\mathfrak{n})(\mathbf{n} - \mathbf{M}_\mathfrak{n})^H\right) \\ &= E(\mathbf{n}\mathbf{n}^H) = \sigma_\mathfrak{n}^2 \mathbf{I}^{(2N_s)}, \end{aligned} \qquad (6)$$

where $\mathbf{0}^{(2N_s)}$ and $\mathbf{I}^{(2N_s)}$ are the $(2N_s \times 1)$-element vector and the $(2N_s \times 2N_s)$-element matrix, respectively.

In Eq. (4), the spreading-code matrix $\mathbf{C}$ is known to the BS and during a specific STBC block interval, the CIR matrix $\mathbf{H}$ can be determined by channel estimation techniques. Hence, given the vector $\mathbf{v}$ in Eq. (4) a particular value $\mathbf{v} \in \mathbb{V}^{(2K)}$ for $i = 1, 2, \ldots, 2^{2K}$, $\mathbf{r}$ in Eq. (1) equals to a random sample $\mathbf{n}$ plus a constant $\xi\mathbf{CHv}$. Hence, by introducing another random vector variable $\mathfrak{r}$ describing the conditional probability of $(\mathbf{r}|\mathbf{C}, \mathbf{H}, \mathbf{v})$ or $(\mathbf{r}|\mathbf{H}, \mathbf{v})$ for short, according to the properties of the complex-valued Gaussian random vector, the PDF of $\mathfrak{r}$ will have the same shape as that of $\mathfrak{n}$, with a mean of $\mathbf{M}_\mathfrak{r} = \mathbf{M}_\mathfrak{n} + \xi\mathbf{CHv}$ and a variance of $\boldsymbol{\Sigma}_\mathfrak{r} = \boldsymbol{\Sigma}_\mathfrak{n}$. Based on the above arguments related to Eq. (6), the conditional PDF can be formulated as

$$\begin{aligned} p(\mathbf{r}|\mathbf{H}, \mathbf{v}) &= \frac{1}{\pi^d} \frac{\exp\left(-\frac{1}{2}(\mathbf{r} - \mathbf{M}_\mathfrak{r})^H 2\boldsymbol{\Sigma}_\mathfrak{r}^{-1}(\mathbf{r} - \mathbf{M}_\mathfrak{r})\right)}{\det(\boldsymbol{\Sigma}_\mathfrak{r})} \\ &= \frac{1}{(\pi\sigma_\mathfrak{n}^2)^{2N_s}} \exp\left(-\frac{1}{\sigma_\mathfrak{n}^2}\|\mathbf{r} - \xi\mathbf{CHv}\|^2\right). \end{aligned} \qquad (7)$$

Hence, the LLRs of the ACO/ST-MUD algorithm are calculated as

$$L_\kappa^{\text{ACO}} = \ln \frac{\sum\limits_{\tilde{\mathbf{x}}_{\kappa+,i}^{(2K)} \in \tilde{\mathbb{X}}_{\kappa+}^{(2K)}} \exp\left(-\frac{1}{\sigma_\mathfrak{n}^2}\|\mathbf{r} - \xi\mathbf{CH}\tilde{\mathbf{x}}_{\kappa+,i}^{(2K)}\|^2\right)}{\sum\limits_{\tilde{\mathbf{x}}_{\kappa-,i}^{(2K)} \in \tilde{\mathbb{X}}_{\kappa-}^{(2K)}} \exp\left(-\frac{1}{\sigma_\mathfrak{n}^2}\|\mathbf{r} - \xi\mathbf{CH}\tilde{\mathbf{x}}_{\kappa-,i}^{(2K)}\|^2\right)},$$
$$i = 1, \ldots, \tilde{x}_\kappa, \;\; \tilde{x}_\kappa \ll 2^{2K-1}, \qquad (8)$$

for $\kappa = 1, 2, \ldots, 2K$. In (8), $\tilde{\mathbf{x}}_{\kappa+,i}^{(2K)}$ and $\tilde{\mathbf{x}}_{\kappa-,i}^{(2K)}$ are $2K$-length binary vectors having elements of $+1$ and -1, for $i = 1, \ldots, \tilde{x}_\kappa$, respectively, while $\tilde{\mathbb{X}}_{\kappa+}^{(2K)}$ and $\tilde{\mathbb{X}}_{\kappa-}^{(2K)}$ are the two sets hosting the two types of vectors that are used for computing the soft outputs and $\tilde{x}_\kappa = \sharp\tilde{\mathbb{X}}_{\kappa\pm}^{(2K)}$ is the number of vectors, i.e. the size of the corresponding two sets.

In the next sections, we will formulate the algorithm of maximizing the value of $\tilde{x}_\kappa$ and that of creating the pool $\tilde{\mathbb{X}}_{\kappa\pm}^{(2K)}$, while imposing a significantly lower complexity than that of the algorithm of calculating all the LLRs employed by the Bayesian detector.

B. Soft-Output ACO-based ST-MUD Algorithm

The soft-output ACO-based ST-MUD algorithm employs the hard-output STBC-assisted twin-transmit antenna DS-CDMA system[1] in

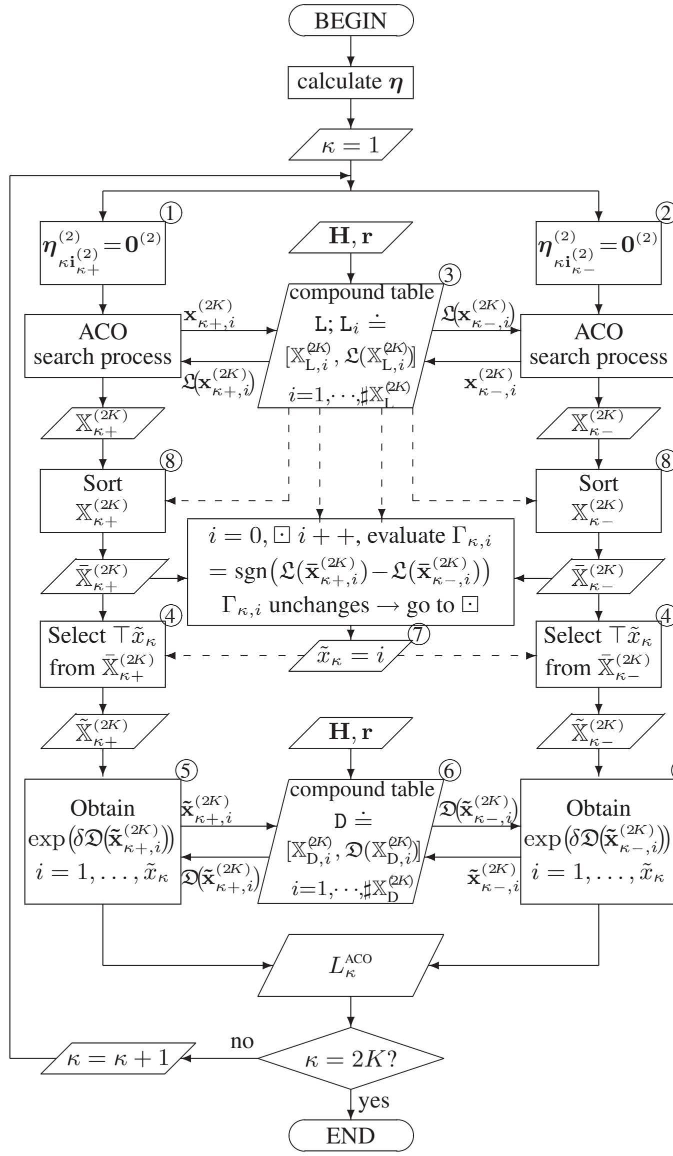

Fig. 2: Flow chart of the SO ACO-based ST-MUD algorithm.

order to generate the two decision candidate pools $\tilde{\mathbb{X}}_{\kappa\pm}^{(2K)}$ containing $2K$-element vectors. Then, based on the two candidate pools $\tilde{\mathbb{X}}_{\kappa\pm}^{(2K)}$ that comprise all the vectors that will be used to calculate the value of L_κ^{ACO}, the LLR of the κth symbol will be calculated according to Eq. (8). Below, we will summarize the actions of the SO ACO-based ST-MUD algorithm using the flow-chart of Fig. 2. The LLR values L_κ^{ACO} of the κth symbol, $\kappa = 1, 2 \ldots K \ldots 2K$, are evalulated in $2K$ consecutive loops of Fig. 2, respectively. However, the $(4 \times K)$-element intrinsic affinity matrix $\boldsymbol{\eta}$, whose value will be utilized repeatedly during the $2K$ loops of Fig. 2 has to be evalulated before the first loop. In order to calculate the value of L_κ^{ACO}, the algorithm is carried out in two parallel branches associated with the κth symbol being $+1$ and -1. More specifically, both branches proceed based on an updated $(4 \times K)$-element intrinsic affinity matrix $\boldsymbol{\eta}_{\kappa+}$ or $\boldsymbol{\eta}_{\kappa-}$, whose value has been obtained before the hard-output ACO search process was activated. As detailed in Steps 1-7 of Fig. 2 and Table I, in order to ensure that the artifical ants generate vectors with the κth symbol being ± 1, the elements in $\boldsymbol{\eta}$ associated with the κth symbol being ∓ 1 have

[1]The hard-output ACO-based ST-MUD algorithm has been proposed in a companion paper submitted to VTC10' Spring, which may be dow-loaded from http://www.ieeevtc.org/vtc2010spring/.

TABLE I: Detailed interpretation of each step in the SO ACO-based ST-MUD algorithms's flow chart of Fig. 2.

Step 1	$\mathbf{i}_{\kappa+}^{(2)} = \begin{cases} [3,4]^T & \text{if } 1 \equiv \kappa \pmod 2 \\ [2,4]^T & \text{if } 0 \equiv \kappa \pmod 2 \end{cases}$
Step 2	$\mathbf{i}_{\kappa-}^{(2)} = \begin{cases} [1,2]^T & \text{if } 1 \equiv \kappa \pmod 2 \\ [1,3]^T & \text{if } 0 \equiv \kappa \pmod 2 \end{cases}$
Step 3&6	The compound table L or D are defined so that each row of them contains two compound elements: the $2K$-element binary vector $\mathbf{x}_{\mathrm{L},i}^{(2K)} \in \mathbb{X}_{\mathrm{L}}^{(2K)}$ and the LLF function $\mathfrak{L}(\mathbf{x}_{\mathrm{L},i}^{(2K)})$ of it or the $2K$-element binary vector $\mathbf{x}_{\mathrm{D},i}^{(2K)} \in \mathbb{X}_{\mathrm{D}}^{(2K)}$ and the Euclidean distance $\mathfrak{D}(\mathbf{x}_{\mathrm{D},i}^{(2K)})$ of it. Each $2K$-element vector is different from all the other $2K$-element vectors in the same table. $\sharp\mathbb{X}_{\mathrm{L}}$ or $\sharp\mathbb{X}_{\mathrm{D}}$ is the cardinality of set $\mathbb{X}_{\mathrm{L}}$ or $\mathbb{X}_{\mathrm{D}}$, which contains all the different $2K$-element binary candidate-vectors whose LLFs or Euclidean distances have been calculated during the current STBC-block duration.
Step 4	$\top\tilde{x}_\kappa$ means the highest ranked $\tilde{x}_\kappa$ number of elements in the ordered set $\tilde{\mathbf{x}}_\kappa^{\pm}$.
Step 5	δ is the coefficient, in this section $\delta = -[\sigma_{\mathfrak{n}}^2]^{-1}$.
Step 7	$\tilde{x}_\kappa = \sharp\tilde{\mathbb{X}}_{\kappa+}^{(2K)} = \sharp\tilde{\mathbb{X}}_{\kappa-}^{(2K)}$ is the cardinality of the two sets $\tilde{\mathbb{X}}_{\kappa\pm}^{(2K)}$ having the same number of members.

to be set to zero. Instead of setting only one entry in the $(2 \times K)$-element intrinsic affinity matrix $\boldsymbol{\eta}$ to zero, which is the case when the system supports K users and employs only one transmit antenna per user, now two entries of the $(4 \times K)$-element intrinsic affinity matrix $\boldsymbol{\eta}$ will be set to zero, because our K-user system employs two transmit antennas for each user with the aid of the $\mathcal{G}_2$ STBC code. More details about the row index associated with the route-table entries are provided in step 1 and 2 of Fig. 2 and Table I. After this update, the search process will be activated based on the value of $\boldsymbol{\eta}_{\kappa\pm}$. The remaining details of calculating the probabilities associated with the entries of the route table, the selection of the artificial ants, the pheromone update algorithms and the termination condition will not be repeated here, since they were detailed in [11].

After the 'ACO search process' of Fig. 2 terminates, the two search pools $\mathbb{X}_{\kappa\pm}^{(2K)}$ generated by the two parallel search processes will continue in the 'Sort', 'Select' blocks numbered as '8' and '4' in order to generate the twin calculation pools $\tilde{\mathbb{X}}_{\kappa\pm}^{(2K)}$, as detailed in [4]. Given the two calculation pools $\mathbb{X}_{\kappa\pm}^{(2K)}$, the Euclidean distance of each vector belonging to the sets $\mathbb{X}_{\kappa\pm}^{(2K)}$ can be obtained and then the resultant LLR value L_κ^{ACO} can be evaluated based on Eq. (8).

The two compound tables L and D of Fig. 2 store the LLF values and the Euclidean distances of the $2K$-symbol binary vectors that have been generated by the artificial ants in the current STBC block duration. More explicitly, the compound element in the first column of every row of the compound table L (or D) is a certain $2K$-symbol vector-value, while the element of the second column records its LLF value (or Euclidean distance) associated with that specific vector-value. The vector-value stored in each row of both tables is unique. These two compound tables are set up to reduce the computational complexity. More specifically, a certain vector-value may be captured by the search pool more than once throughout the entire ACO-based search procedure activated once during each STBC block interval. However, the LLF or the Euclidean distance value associated with any vector-value does not have to be calculated more than once. By recording all the unique vector-values captured during a STBC block interval in L and D, any redundant computations associated with the repeated calculation of the LLF or Euclidean distance of the same vector-value can be avoided. Additionally, all the contents in the two compound tables have to be cleared, when the soft-output ACO-based STBC-MUD algorithm was concluded for a specific STBC block duration.

IV. Performance Results

In this section, we consider the K-user DS-CDMA UL employing two transmit antennas and a single receive antenna in order to demonstrate the performance improvements achieved by the SO-ACO based ST-MUD employed in the system proposed in Fig. 1. The system of Fig. 1 employs a URC encoder, RSC encoder, STBC encoder and DS-CDMA spreading at each MS's transmitter in conjunction with the SO-ACO based ST-MUD and the per-user URC as well as RSC decoder at the BS's receiver. All simulation parameters are listed in Table. II.

TABLE II: Parameters for the RSC-coded and URC precoded STBC-CDMA system employing the SO-ACO based ST-MUD algorithm.

System	Modem	BPSK
	Multiple access mothod	DS-CDMA
	Spreading code	Gold code
	Spreading factor	$N_{\mathrm{s}} = 31$
	No. of transmit antennas	2
	No. of receive antennas	1
	No. of users	K=1,10,20,32
	Channnel	Uncorrelated Rayleigh fading
RSC	Code rate	1/2
	Constraint length	3
	Feedback generator	5
	Feedforward generator	7
URC	Constraint length	2
	Feedback generator	3
	Feedforward generator	2
SO-ACO/ ST-MUD	Initial pheromone	$\tau = 0.01$
	Evaporation rate	$\rho = 0.5$
	Number of ants	$\zeta = 10$
	Number of iterations	$\Xi = 10$
	Weight of pheromone	$\alpha = 1$
	Weight of intrinsic affinity	$\beta = 6$
	Weight for the elite ant	$\sigma = 8$
Interleaver	Type	random
	size	N_{c}=$2{\times}10^1$,10^2, 10^3,10^4 bits

As observed from Fig. 3, when $K = 32$ users are supported by the system employing the parameters of Table. II, the BER performance of the $K = 32$-user system approaches that of the single-user system within less than 0.01 dB. However, the complexity of the SO-ACO based ST-MUD algorithm that detects the $2 \times 32 = 64$ STBC symbols transmitted by the $K = 32$ users within each STBC-block duration is significantly lower than that of the optimal Bayesian algorithm. More quantatively, the number of Euclidean distance evaluations imposed by the SO-ACO based ST-MUD algorithm within a STBC-block duration for $K = 32$ users is as low as about 10^3, which is a fraction of 10^{-17} compared to the 10^{20} evaluations required by the Bayesian algorithm.

V. Conclusion

We proposed a URC-precoded, 1/2-rate RSC-and STBC-coded three stage concatenated multiuser DS-CDMA system, where each user is equipped with a twin-transmit-antenna, which enables each user to achieve an effective throughput of 0.5 bit/s/Hz within about 0.5 dB of the single-user E_{b}/N_0 limit. The following observations can be made from the results obtained. Firstly as expected, a second-order diversity gain has been achieved by the twin-transmit-antenna system.

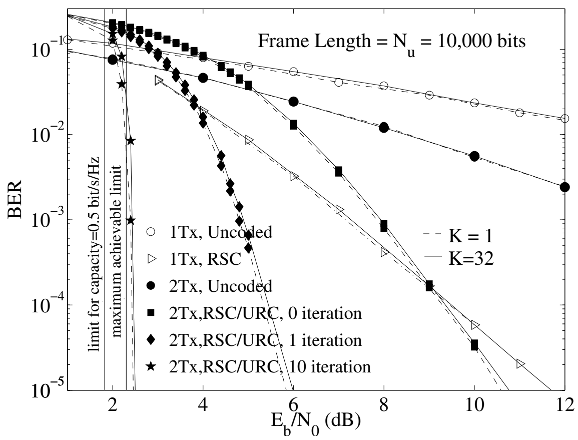

Fig. 3: Performance comparison of the URC-precoded and non-precoded RSC-coded twin-antenna-aided or single-antenna aided DS-CDMA system for $K = 1$ and $K = 32$ users supported by the system employing the SO-ACO based ST/MUD algorithm and using the system parameters outlined in Tab. II. The interleaver length was $N_c = 20,000$ bits, and the 1/2 rate RSC code was employed to encode every input frame having a length of $N_u = 10,000$ bits.

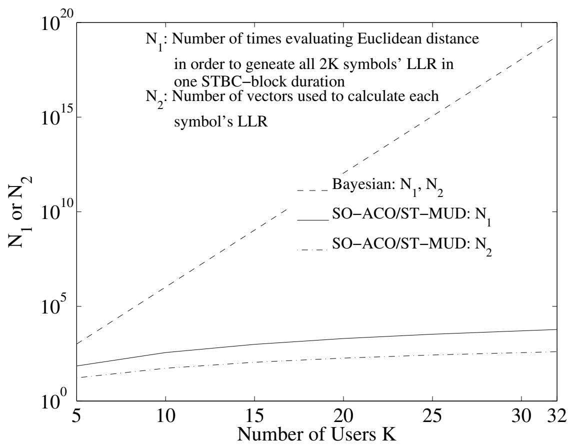

Fig. 4: Complexity comparison of the SO-ACO based ST-MUD algorithm and of the Bayesian algorithm plotted versus the number of users supported by the twin-antenna-aided system.

Additionally, by employing the proposed SO-ACO based ST/MUD at the BS' receiver in conjunction with Gold-codes having a length of 31 chips, up to $K = 32$ users may be supported at a trivially increased E_b/N_0 requirement, while achieving the same BER performance as the single user system employing the same number of MUD/decoding iterations. The system's complexity was about 10^{17} lower than that of the Bayesian detector.

References

[1] A. Colorni, M. Dorigo and V. Maniezzo, "Distributed optimization by ant colonies," in *Proceedings of the European Conference on Artificial Life*, 1991, pp. 134–142.

[2] S. L. Hijazi and B. Natarajan, "Novel low-complexity DS-CDMA multiuser detector based on ant colony optimization," in *Proceedings of IEEE Vehicular Technology Conference*, vol. 3, 2004, pp. 1939–1943.

[3] C. Xu, L.-L. Yang, R.-G. Maunder and L. Hanzo, "Near-optimum soft-output ant-colony-optimization based multiuser detection for the DS-CDMA uplink," in *Proceedings of the IEEE International Conference on Communications*, 19-23, May, 2008, Beijing, China, pp. 795–799.

[4] C. Xu, R. G.Maunder, L.-L. Yang and L. Hanzo, "Near-optimum multiuser detectors using soft-output ant-colony-optimization for the DS-CDMA uplink," in *IEEE Signal Processing Letters*, vol. 57, pp. 137–140, February, 2009.

[5] L. Hanzo, O. Alamri, M. E.-Hajjar and N. Wu, *Near-Capacity Multi-Functional MIMO Systems* John Wiley and Sons, USA: 2009.

[6] A. Sezgin, D. Wuebben and V. Kuehn, "Analysis of mapping strategies for turbo-coded space-time block codes," in *Proceedings of IEEE Information Theory Workshop*, (Paris,France), pp. 103-106, March/April 2003.

[7] S. Benedetto, D. Divsalar, G. Montorsi and F. Pollara, "Serial concatenation of interleaved codes: performance analysis, design, and iterative decoding," in *IEEE Transactions on Information Theory*, vol. 44, pp. 909-926, May 1998.

[8] D. Divsalar, S. Dolinar, F. Pollara, "Serial concatenated trellis coded modulation with rate-1 inner code," in *IEEE Global Telecommunications Conference (GLOBECOM)*, vol. 2, (San Francisco, CA), pp. 777-782, 2000.

[9] S. ten Brink, "Convergence of iterative decoding, *Electronics Letters*, vol. 35, no. 10, pp. 806808, May, 1999.

[10] S. M. Alamouti, "A simple transmit diversity technique for wireless communications,"*IEEE Journal on Select Areas in Communications*, vol. 16, No. 8, pp. 1451–1458, Oct. 1998.

[11] C. Xu, L.-L. Yang and L. Hanzo, "Ant-colony-based multiuser detection for MC DS-CDMA systems," in *Proceedings of the IEEE Vehicular Technology Conference*, 30, Sep-3, Oct, 2007, Baltimore, MD, USA, pp. 960–964.

[12] J. Hagenauer, "The EXIT chart - Introduction to extrinsic information transfer in iterative processing," in *Proceeding of the European Signal Processing Conference*, Vienna, Austria, pp. 1541-1548, September 2004.

[13] S. Kay, *Fundamentals of Statistical Signal Processing, Estimation Theory*. New Jersey, USA: Prentice Hall, 1993.